Science of the Total Environment 666 (2019) 652–661

Contents lists available at ScienceDirect

Science of the Total Environment

journal homepage: www.elsevier.com/locate/scitotenv

The role of air pollution and climate on the growth of urban trees

Giuliano Maselli Locosselli [a,b], Evelyn Pereira de Camargo [a,b], Tiana Carla Lopes Moreira [d], Enzo Todesco [c], Maria de Fátima Andrade [c], Carmen Diva Saldiva de André [e], Paulo Afonso de André [d], Julio M. Singer [e], Luciana Schwandner Ferreira [f], Paulo Hilário Nascimento Saldiva [b,d], Marcos Silveira Buckeridge [a,b,*]

[a] Instituto de Biociências, Universidade de São Paulo, São Paulo, Brazil
[b] Instituto de Estudos Avançados, Universidade de São Paulo, São Paulo, Brazil
[c] Instituto de Astronomia e Geofísica, Universidade de São Paulo, São Paulo, Brazil
[d] Faculdade de Medicina, Universidade de São Paulo, São Paulo, Brazil
[e] Instituto de Matemática e Estatística, Universidade de São Paulo, São Paulo, Brazil
[f] Faculdade de Arquitetura e Urbanismo, Universidade de São Paulo, São Paulo, Brazil

HIGHLIGHTS

- Spatial/temporal variability of urban climate and air pollution affect tree growth.
- Despite heat island effects, trees grow faster under warmer conditions
- Despite water limitation by impervious cover, precipitation does not affect growth.
- Air pollution (Al, Zn, Ba, PM_{10}) has a stronger influence than climate on growth.
- Cities can affect tree development and interfere with adaptation to climate change.

GRAPHICAL ABSTRACT

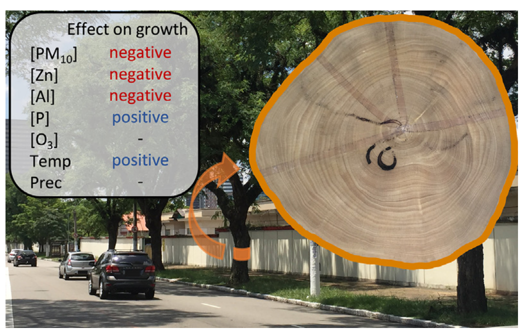

ARTICLE INFO

Article history:
Received 21 December 2018
Received in revised form 13 February 2019
Accepted 18 February 2019
Available online 19 February 2019

Editor: Elena Paoletti

Keywords:
Tree ring
Dendrochronology
Particulate matter
Mitigation
Climate change
Ecosystem services

ABSTRACT

The urban environment features poor air quality and harsher climate conditions that affect the life in the cities. Citizens are especially vulnerable to climate change, because heat island and impervious exacerbates extreme climate events. Urban trees are important tools for mitigation and adaptation of cities to climate change because they provide ecosystem services that increase while trees grow. Nonetheless, the growth of trees may be affected by the harsher conditions found in the urban environment. We assessed the impact of air pollution and climate on the spatial/temporal variability of tree growth in São Paulo, Brazil, one of the largest urban conglomerates in the world. For this purpose, we sampled 41 trees of the *Tipuana tipu* species in a region that includes industrial areas. We built a tree-ring chronology using standard dendrochronological methods. Spatial analyses show that trees grow faster in the warmer parts of the city and under higher concentrations of airborne P, whereas growth is reduced under higher concentrations of Al, Ba, Zn. Particulate matter (PM_{10}) from the industrial cluster also reduce average growth rate of trees, up to 37% in all diameter classes. Similar results were obtained via temporal analyses, suggesting that the annual growth rate is positively associated with temperature, which explain 16% of interannual growth variability. Precipitation, on the other hand, has no association with tree growth. The average concentration of PM_{10} explains 41% of interannual growth variability, and higher concentrations during the driest months reduce growth rate. Despite heat island effect and water limitation in the soil of the city, this

* Corresponding author at: Department of Botany, Institute of Biosciences, University of São Paulo, São Paulo, SP, Brazil.
E-mail address: msbuck@usp.br (M.S. Buckeridge).

https://doi.org/10.1016/j.scitotenv.2019.02.291
0048-9697/

species takes advantage of warmer conditions and it is not limited by water availability as measured by precipitation. On the other hand, air pollution directly impacts the growth of these trees being a major limiting growth factor.

1. Introduction

Poor air quality and harsher climate conditions are significant issues in the cities affecting human health and well-being. Citizens face high levels of air pollution in the megacities, where particulate matter concentrations are few folds higher than the recommended levels by the World Health Organization (Cheng et al., 2016). Urban population is also considered to be vulnerable to the effects of climate change, because heat islands and impervious cover, among other factors, exacerbate the effects of extreme climate events in cities (Hunt and Watkiss, 2011). Urban trees play an important role in the reduction of air pollution and the adaptation and mitigation to climate change through their ecosystem services. They include the capacity of: filtering air pollution (Escobedo and Nowak, 2009; Manes et al., 2012; Sicard et al., 2018), assimilating CO_2 (Nowak et al., 2013), regulating air temperature (Livesley et al., 2016), mitigating storm-water runoff (Xiao and McPherson, 2002; Livesley et al., 2016), producing and probably controlling humidity (Buckeridge, 2015), and providing recreational, social, psychological and aesthetic benefits (Smardon, 1988). On this basis, urban trees are considered as one of the main means of adaptation to climate change in cities (de Coninck et al., 2018). These potential ecosystem services increase as trees grow and get bigger (McPherson et al., 1994; Sydnor and Subburayalu, 2011; Mullaney et al., 2015). However, air pollution and climate change themselves may affect tree development (Ordóñez and Duinker, 2014). The senescence of urban trees can become an economic burden to cities due to the costs associated with removing dead specimens, accidents caused by the fall of trees, and the reduction of their ecosystem services (Brandt et al., 2016).

Climate is one of the most important modulators of tree growth around the world, evidencing their vulnerability to climate change (Hughes, 2002). The influence of climate on the growth of trees can be accurately assessed by tree-ring analyzes (Schweingruber, 1988). This approach, named dendrochronology, has mainly been used to understand the climate/growth relationships in the natural environment (Hughes, 2002), but to a lesser extent in the urban landscape (e.g., Bartens et al., 2012; Gillner et al., 2014). Less favorable urban climate conditions (Hunt and Watkiss, 2011) may increase the vulnerability of tree development to climate change.

In addition to climate, the complexity of the urban environment includes other anthropogenic factors that may also influence tree growth. Additional effects of air pollution should be expected (Ordóñez and Duinker, 2014) as it may influence tree development. Ozone (O_3), particulate matter (PM_{10}) and the related metal composition are known to influence tree development through changes in optical properties of leaves by adsorption of PM_{10}, and direct effect of PM_{10} and O_3 on photosynthetic systems and stomatal functioning (Paolletti, 2013; Grantz et al., 2003; Prajapati, 2012). Such damages to the gas-exchange and assimilation systems have the potential to impact tree growth.

Our objective was to evaluate how climate and air pollution modulate the growth of urban trees. For this purpose, we studied the tree rings of one of the most common tree species in the metropolitan region of São Paulo, namely *Tipuana tipu* (Benth.) Kuntze, a deciduous broadleaf species. This species is known for providing some ecosystem services as filtering air pollution by accumulating airborne Al, Ba, Cu, Mn, Fe, S and Zn in their barks (Moreira et al., 2018), and in the tree rings (Locosselli et al., 2018). This species also reduces heat island effect by attenuating up to 80.2% of solar radiation (Abreu-Harbich et al., 2015).

We considered the following hypotheses in this study: I) the average growth rate of urban trees depends on the spatial variability of microclimate and air pollution levels found across the city landscape; II) the interannual variability of growth rate of urban trees depends on the temporal variability of climate and air pollution levels; III) climate has a greater influence on the growth rate of trees than air pollution, as it is one of most important drivers of interannual growth variability in natural areas.

2. Material and methods

2.1. Study site

Sampling took place in the metropolitan region of São Paulo, Brazil, one of the largest urban conglomerates in the world, with >20 million inhabitants (UN, 2018). We chose an area that combines a typical urban landscape in the vicinity of a significant industrial cluster. This region (Capuava, Supplementary Material Fig. S1) is located at 23° 38′S and 46° 28′W, 700 m above sea level. It is a complex landscape that includes industrial, commercial and residential areas, all under the influence of a heterogeneous vegetation cover (Fig. 1A). Traffic intensity also varies from local to express streets. The industrial companies are mainly concentrated in a large area in the center of our study site (Fig. 1A). They comprise mainly oil refineries, but also cement and fertilizer plants. The industrialization process began in the 1950's, with the construction of the main oil refinery. The climate of the sampling site is tropical to sub-tropical with a dry season during winter. It has a mean annual temperature of 20 °C and 1726 mm of total annual precipitation (Fig. 1B).

2.2. Species and sampling methodology

We sampled trees of the *Tipuana tipu* (Benth.) Kuntze, Fabaceae. The presence of this species is not only restricted to Brazilian cities; it is also found in Argentina, United States, Portugal, South Africa, Israel, among others (Breuste, 2013; Mazza et al., 2013; Teixeira, 2014; Legumes, 2017; Kuruneri-Chitepo and Shackleton, 2011; Soares et al., 2011; Sashua-Bar et al., 2010; Moreira et al., 2018). It is a deciduous species (Zaproni et al., 2013) that reaches up to 20 m of height and one meter of diameter at breast height (DBH) in São Paulo. This species produces well defined semi-ring porous tree rings delimited by the presence of marginal parenchyma (Supplementary Material, Fig. S2).

In August 2016, we sampled 41 trees using 5 mm increment borers, from two to three increment cores per tree, totalizing 84 increment cores. All samples were taken at breast height (DBH, about 1.3 m from topsoil). Samples were never obtained over apparently damaged parts of the trunk or over reaction wood. We avoided trees with the presence of scars, heavy pruning or with the base of the stem constricted by the sidewalk. Tree height, DBH, conditions of growth and geographical position were recorded for all trees. We used a saturated solution of copper sulfate and calcium oxide in the injuries to avoid fungi. All samples were fixed in wooden supports and left to dry for a couple of weeks.

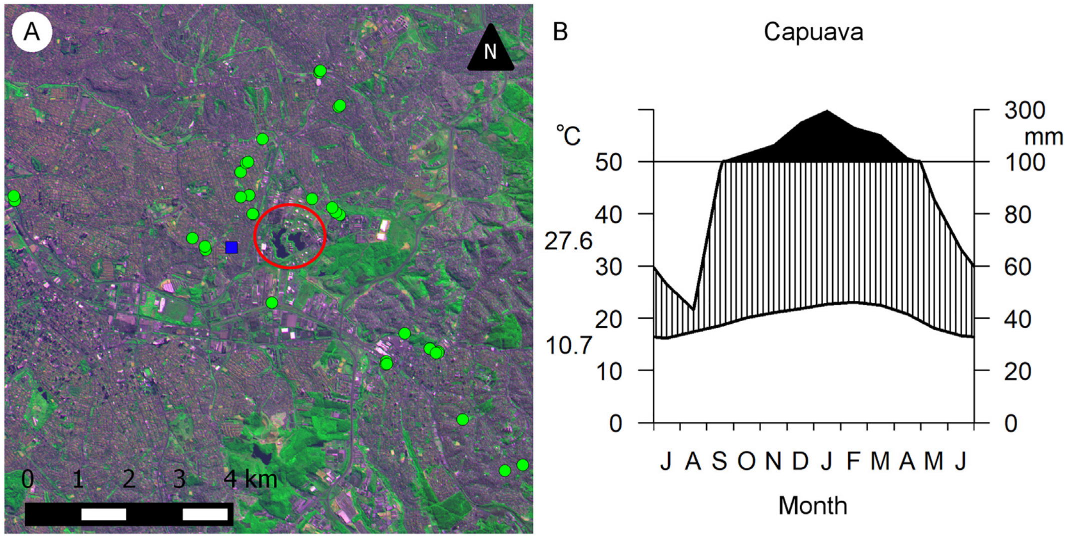

Fig. 1. Sampling site characteristics. A) RGB image of the sampling site (CBERS 4, July 10th 2016, purple indicates concrete, and green indicate green areas) showing the location of all sampled trees (green circles). The air quality station of the Environmental Company of São Paulo State (CETESB) is represented as a blue square. B) Climate diagram of the sampling site showing a dry season between June and August. Average maximum and minimum temperatures are shown in the temperature axis.

2.3. Sample preparation and tree-ring analyses

Samples were polished using sandpaper with different grits (from 50 to 600). All samples were cleaned with pressurized air to remove the wood powder from the vessel lumen. Tree rings were identified and marked under a stereomicroscope and they were measured using the Lintab 6 system (Rinntech Germany). Samples of seven trees were removed from the study because they were at advanced stages of decay with non-visible tree-ring boundaries. Tree rings were visually crossdated by analyzing the year-to-year tree-ring width variability to identify common growth patterns and to accurately date the year of formation of each tree-ring (Stokes and Smiley, 2006). We first crossdated the different radii of the same tree to look for missing and false rings. We then crossdated the radii of different trees using the TASP-Win software. We checked the dating quality using the COFECHA software (Holmes, 1993). We also removed an additional five trees that showed low correlation values with the master dating chronology of COFECHA in order to improve the common growth signal (Brienen and Zuidema, 2005).

The final tree-ring chronology was built using the ARSTAN software (Cook and Kairiukstis, 1990; Cook and Holmes, 1996). All tree-ring series were de-trended with a 10-year cubic smoothing spline function in order to remove biological trends from the tree-ring series (Cook and Kairiukstis, 1990). We chose a 10-year window because the sampled tree-ring series were on average 29 years long. The standard tree-ring chronology, which retains part of the auto-correlation, was used in the present study. The expressed population signal (EPS, Wigley et al., 1984) and the r-bar were calculated using the ARSTAN software.

Since we missed the pith in some cores while sampling, we estimated the position of the pith to calculate the number of missing tree rings. For this purpose, we scanned all samples at 1200 dpi (EPSON V-30) and drew parallel lines to the rays in the innermost part of the samples using the GIMP software (version 2.8.10). The convergence point of these lines is the estimated position of the pith. The number of missing tree rings in the samples was estimated by dividing the distance to the pith (measured with the Image J software, Schneider et al., 2012) by the average width of the innermost five tree rings (modified from Hietz, 2011). This analysis is needed to accurately calculate the growth rate of each tree using basal area increment and diameter growth rate by stem diameter class. Both were used as a measure of tree growth in this study to compensate for the differences in the DBH of the sampled trees.

2.4. Spatial variability of growth

We evaluated the influence of spatial variability of microclimate and air pollution on the growth rate of *T. tipu* trees. For short-term effects, we evaluated the association between the response variable: mean basal area increment (BAI) of the last ten years (computed as the mean annual increment in an area of the transversal section of the stem), and the following predictor variables: surface temperature (as a measure of micro-climate) and concentration of airborne metals. For the long-term effects, we evaluated the association between the response variable: average diameter growth rate controlling for diameter class, and the following predictor variables: site characteristics (trees growing in parks or sidewalks) and the modeled emissions of PM_{10} from the industrial cluster.

2.4.1. Short-term effects

Spatial variability in surface temperature was calculated using temperature data obtained from the Landsat 8 infrared thermal band (at 30 m resolution). For this analysis, we used the February 16th, 2017 image that corresponds to the month with the best correlation between mean air temperature and tree-ring index (refer to the results for further details). This satellite image was obtained from the United States Geological Service and was analyzed using the ENVI 5.1 software (Harris Geospatial Solution). We first computed the spectral radiance from the image grey levels (USGS, 2018), and proceeded with the atmospheric corrections (Barsi et al., 2003). Values of atmospheric transmittance, emitted radiance and incident radiance were obtained from NASA for the “Mirante de Santana (SP)” Station (National Institute of Meteorology, Brazil). Finally, we converted radiance values to surface temperature (°C) at 30 m resolution (USGS, 2018). All equations and correction data are provided in the supplementary material.

Concentrations of metal elements that compose air pollution were estimated using the barks of the sampled trees as biomonitoring tools. Chemical elements in tree barks are associated with the composition of air pollution (Cocozza et al., 2016; Moreira et al., 2016). Tree barks have been largely used to access recent local air pollution variability, and *Tipuana tipu* stands out as a reliable biomonitoring species (Moreira et al., 2018). For this purpose, we collected four 8 cm × 8 cm samples of the periderm of each tree using titanium tools to prevent contamination. All bark samples were dried in an oven at 60 °C for 48 h and later cleaned using a nylon toothbrush. All cleaned samples

had their outermost 3 mm (corresponding to the outermost periderm) grated with a titanium tool. Tree bark samples were then ground to powder on a micro-mill with agate mortar (Fritsch Pulverisette 0, Fritsch GmbH, Idar-Oberstein, DE). The periderm powder was later compressed using a hydraulic press with a pressure of 3.9 ton/cm^2. Boric acid (H_3BO_3, p.a. ACS reagent) was used as the base for the pellets. The chemical composition of the barks was obtained via an energy dispersive X-ray fluorescence spectrometer - EDXRF (EDX 700 - HS, Shimadzu Corp., Kyoto, Japan) with the standard Peach Leaves #1547 (National Institute of Standards and Technology (NIST), Gaithersburg, MD, USA). We analyzed the concentration of the following chemical elements related to traffic intensity, biomass burning and biofuel: Al, Ba, P, Zn. (Moreira et al., 2016).

To evaluate the combined effects of surface temperature and airborne concentrations of metals on the growth of trees, we used principal component analyses to reduce the data dimensionality and linear regression models to evaluate the association between BAI and the first and second components. We included the age of the trees as an additional variable in the regression models, because BAI may not be entirely independent of age.

2.4.2. Long-term effects

To evaluate the isolated effects of the industrial cluster emissions on the growth of trees, we used AERMOD to model the spatial distribution of airborne PM_{10}. The use of Weather Research Forecast (WRF) model combined with the AERMOD dispersion model has been used to identify the influence area of the sources and to calculate the isopleths of pollutants concentration (Kumar et al., 2016). The model calculates the data according to the air quality standards, that are 24 h average for the PM_{10}. The average concentration is calculated for each grid cell of the receptor grid (Supplementary Material, Fig. S3). Meteorological fields were provided by the WRF model as input to the calculation performed by the AERMOD model (Afzali et al., 2017). In this work it was only considered the contribution from the Capuava petrochemical industry to the emission of particles and gaseous compounds. The emission inventory was provided by the Petrochemical Industry to the Environmental Company of the State of São Paulo (CETESB). We considered the model output to define three categories of exposure to annual PM_{10} emissions based on the concentration isopleths: low (0.05–0.09 μg/m^3), medium (0.10–0.49 μg/m^3), and high (0.50–0.80 μg/m^3). We also categorized the trees as either growing in sidewalks or in public parks.

In order to evaluate the combined association of tree growth and exposure with industrial emissions and site characteristics, we considered linear mixed effects regression models. Since these variables may have a long-term effect on the sampled trees, we included diameter class - from 10 cm to 50 cm of DBH in 10 cm intervals (Peters et al., 2015) as an additional variable. Diameter class, industrial emissions and site characteristics as well as possible interactions among them were considered as explanatory variables. The diametric growth rate was adopted as the response variable. The final model contains only the statistically significant variables ($\alpha = 0.05$).

2.5. Temporal variability of growth

In addition to the analyses of spatial variability of growth rate, we assessed the influence of climate and air pollution on the year-to-year growth variability. We used the built standard tree-ring chronology to evaluate the influence of annual variability of climate and air pollution on the growth of *T. tipu* trees.

For the climate/growth analyses, we considered the climate data from the Climate Research Unit (version 4.0 data at 0.5° resolution) obtained at Climate Explorer (Trouet and Van Oldenborgh, 2013). Climate/growth relationships were tested using Pearson's correlation between tree-ring index from the standard chronology and either monthly temperature or precipitation values from current and past growing seasons.

Similar analyses were performed using air pollution data. The time series for the concentrations of O_3 and PM_{10} were obtained with the QUALAR tool from the Environmental Company of the State of São Paulo (http://cetesb.sp.gov.br/ar/qualar/). The average values of PM_{10} and O_3 in this site are 35.53 μg / m^{-3} and 35.77 μg / m^{-3} for the available period, respectively. We detrended the series with a 10-year cubic smoothing spline function to remove long-term trends found in the data of air pollution (Supplementary Material Figs. S4 and S5). The corresponding residuals retain mostly the high-frequency variability that is more adequate to evaluate its correlation with the standard tree-ring chronology. The analysis was conducted for four periods: January to December, corresponding to the end of the previous growing season and the beginning of the current one; June to July +1, representing a growth year; April to September, representing the six driest months; and October to March +1, representing the six wettest months.

We also analyzed the combined effects of climate and air pollution on the interannual growth rate variability of the studied trees. For such purpose, we used linear models with the standard tree-ring chronology as the response variable and climate and air pollution as predictors. We only used variables with the highest correlation values with the tree-ring chronology as predictors. Different models were evaluated and the best one was selected via second order Akaike's Information Criteria (AICc) that is corrected for smaller samples. Residuals were checked for normality and homoscedasticity (Faraway, 2005). All analyses were performed using R (R Core Team, 2017) and the package "AICcmodavg" (Mazerolle, 2017).

3. Results

3.1. Spatial variability of growth rate

The DBH of the sampled trees varied from to 22 cm to 110 cm. The estimated mean age, correcting for missing pith, of the sampled trees is 36 years, ages of the individual trees ranging from 24 to 49 years, while the average growth rate of these trees is 6.57 mm per year (Table 1).

The Principal Component Analysis including the variables: tree age, temperature, and concentrations of airborne Al, Ba, P and Zn resulted in two principal components with eigenvalues higher than 1, which together account for 77% of the data variability (Table 2). The first principal component combines the effects of surface temperature (that varies from 28 to 40 °C in the sampling site, Fig. 2A), and the concentrations of Al, Ba, P and Zn in the bark of the trees (Table 2, Fig. 2B). The second principal component accounts mainly for the variation in tree age. Both components are significantly associated with the average 10-year

Table 1
Diagnostic of the standard tree-ring chronology of *Tipuana tipu*, showing the number of individuals used in the final chronology, the time span of the chronology, average length of individual series in years, the series inter-correlation that is a measure of the strength of the signal, mean sensitivity that is a measure of the variance of tree-ring width, the expressed population signal that is a measure of how well represented is the common growth signal, and the r-bar that is the mean correlation between all series.

Number of trees (radii)	29 (48)
Time span	1975–2015
Average length (years)	29
Average tree-ring width (mm)	6.57
Series intercorrelation[a]	0.47
Mean sensitivity	0.46
Expressed population signal	0.91
r-bar	0.22

[a] From COFECHA.

Table 2
Results of the principal component analysis based on correlation matrix using the following variables: concentration of Al, Ba, Zn and P in tree barks, surface temperature and the age of the sampled trees. Eigenvalues, proportion of explained variance and cumulative proportion are presented for each principal component, as well as the scores of each variable.

	PC1	PC2	PC3
Eigenvalue	3.49	1.13	0.74
Proportion	0.58	0.19	0.12
Cumulative	0.58	0.77	0.89
Variable			
Al	0.51	−0.21	−0.10
Ba	0.51	−0.21	0.07
Zn	0.36	0.03	0.84
P	−0.38	−0.31	0.37
Surf. Temp.	−0.45	−0.03	0.35
Age	0.08	0.90	0.11

BAI (a similar result holds for BAI averages based on the last two to nine years, Supplementary Material, Fig. S6). The BAI tends to decrease with increasing PC2, or when trees get older (Table 3, $R^2 = 0.24$, $p = 0.002$). Also, there is a positive association between the BAI and PC1 (Table 3, $R^2 = 0.19$, $p = 0.005$), showing that temperature and concentrations of airborne P stimulate growth, while higher concentrations of airborne Ba, Zn and Al decrease growth rate.

We also evaluated the combined effects of site conditions (sidewalks vs park) and exposure to industrial PM_{10} emissions on growth rate controlling for diameter class. The growth rates of trees placed in sidewalks and parks are not statistically different (Supplementary Material S7). There is no direct effect of site conditions ($p = 0.29$), of the interaction between site conditions and exposure ($p = 0.23$), nor of the interaction between site and diameter class ($p = 0.43$). However, the mixed effects models indicate significant differences (Table 4) in the growth rate by diameter class of trees growing under different exposures to PM_{10} (see Figs. 3 and S7 for further details in tree position within the dispersion plume). Trees growing in areas under higher exposure to PM_{10} (0.50–0.80 μg/m^3) displayed lower growth rates for all diameter classes when compared to trees growing in areas under medium (0.10–0.49 μg/m^3, $p = 0.03$) or low exposures to PM_{10} (0.05–0.09 μg/m^3, $p = 0.004$). These results show that increasing PM10 by three folds (high x medium

Table 3
Results of the regression analysis between mean basal area increment of the last 10 years and the two principal component analysis. The first principal component accounts for the variation of the concentrations of Al, Ba, Zn, P and the surface temperature, while the second principal component accounts for the variation of trees age.

Variable	DF	Coef (SE)	Contribution (%)	p-Value
Constant		82.12 (4.46)	–	–
PC 1 ([Al], [Ba], [P], [Zn], Temp)	1	−7.41 (4.43)	19.44	0.005
PC 2 (age)	1	−14.51 (4.26)	24.20	0.002
Error	27	–	56.35	–
Total	29	–	100	–

exposures) reduces growth rate by 37%. On the other hand, growth rates are not statistically different between trees growing under medium and low exposures to industrial air pollution ($p = 0.87$) controlling for diameter class.

3.2. Temporal variability of growth rate

In addition to the association between the average growth rate of trees and microclimate and air pollution, we also evaluated the influence of both climate and air pollution on inter-annual growth. For this purpose, we built a tree-ring chronology based on the growth of 29 trees and 48 radii (Table 1, Fig. S8). The final standard chronology ranges from 1975 to 2015, with an inter-series correlation of 0.47 and a mean sensitivity of 0.46. The r-bar is 0.22 and the mean expressed population signal (EPS) is 0.91, above the threshold of 0.85. Despite the high mean EPS value, we only used the chronology segment from 1982 to 2015 because the previous period is only represented by a few series (Supplementary Material Fig. S9).

The inter-annual growth rate (represented here by the tree-ring index) of *T. tipu* is not significantly associated with monthly precipitation in this study area (Fig. 4A). On the other hand, the mean temperature of the previous growth year is negatively associated with the growth of *T. tipu* during the months of August and March (Fig. 4A). The growth rate is positively associated with mean temperature during February of the current growth season (Fig. 4A). Similar associations with mean temperature were found for January ($p = 0.07$) and March ($p = 0.06$), but they were not statistically significant. Association with the average temperature from January to March is statistically

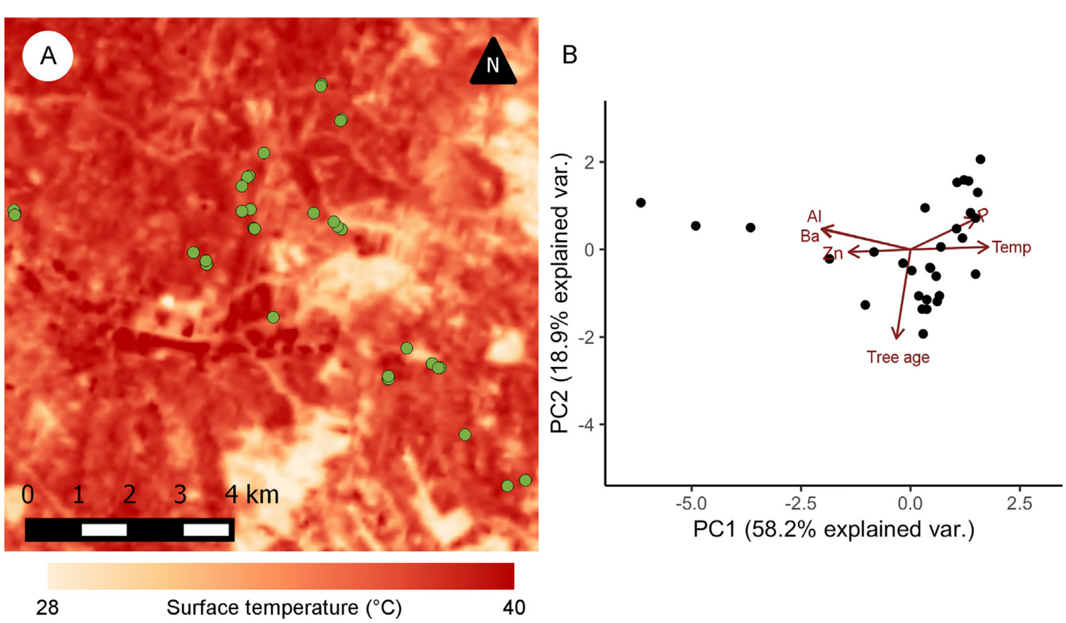

Fig. 2. A) The surface temperature in the sampling site with the location of the sampled trees of *Tipuana tipu* (green circles). Surface temperature calculated based on the Landsat 8 thermal image from February 16th, 2017 B) Plot of the principal component analysis using surface temperature, the concentrations of Al, Ba, Zn, P in the bark of the sampled trees, and the age of the sampled trees.

Table 4
Results of the linear mixed effect model showing the effects of exposition to the emitted PM_{10} and diameter classes on the diametric growth rate of trees. The multiple comparison using Tukey Contrasts is also provided to compare the effects of high, medium and low exposures on growth rate.

Variables	DF	F-value	p-value
Exposition	2	3.49	0.04
Diameter class	4	24.63	< 0.0001
Comparison of means	Estimated Std	z-value	p-value
High - Low	7.29	2.48	0.03
High - Medium	8.62	2.73	0.004
Medium - Low	1.32	2.63	0.87

significant and stronger than with the individual months ($r = 0.46$ and $p = 0.007$, Fig. 4B). Years with lower mean temperature values for this period, which represent the middle of the growing season, are well synchronized with lower tree-ring indexes of *T. tipu*, as warmer years are synchronized with higher growth rates (Fig. 4B).

The inter-annual variability of air pollution is also associated with the annual growth rate of these trees. We evaluated the association between tree-ring indexes and average concentrations of O_3 and PM_{10} (Fig. 5) using Pearson correlation coefficients. These differences in the time-span reflect the data availability. The results show that the growth rate is not significantly associated with O_3 concentrations in any period, while the mean annual concentrations of PM_{10} is significantly associated with the standard tree-ring chronology (Fig. 5A). This association is negative with mean concentrations of PM_{10} for the period between January to December ($r = -0.64$, $p = 0.004$) and during the six drier months of the year from April to September ($r = -0.56$, $p = 0.02$). For both periods, growth rate decreases with higher concentrations of PM_{10}. Correlation is, however, positive with the six wettest months of the year from October to March ($r = 0.56$, $p = 0.02$).

Since both temperature and PM_{10} are significantly associated with the annual growth rate of the sampled trees, we evaluated their combined effects using linear models. We only considered the mean temperature from January to March, and the mean PM_{10} concentrations from January to December. The other variables were not included because of collinearity issues. The best model, with a difference in AICc values higher than 2, includes both temperature and PM_{10} (Table 5). This model explains 57% of the annual growth variability for the period from 1988 to 2015, which corresponds to the length of the PM_{10} series. During this period, annual variability of PM_{10} explains 41% of the growth rate variability of *T. tipu*, while mean temperature explains 16% of this species growth rate variability (Table 5).

4. Discussion

Tipuana tipu produces distinct tree rings well-suited for dendrochronological studies in the urban environment (Locosselli et al., 2018). They are delimited by the presence of marginal parenchyma, with very few false rings. Whenever present, these false rings, characterized by the confluent paratracheal parenchyma, are easily identified because this species features semi-ring porous wood. These trees also show a common growth variability that aided crossdating (Torbenson, 2015), with clear pointer years (years represented by narrow tree rings in all sampled trees) like 1980, 1990, 1995, 1999, 2007, 2012. It is important to note that the presence of impermeable sidewalk cover does not influence the results discussed here. Overall, we found consistent effects of climate and air pollution on the growth rate of *Tipuana tipu* in both spatial and temporal dimensions.

The average growth rate of these trees depends on the spatial and temporal variability of temperature. Surface temperature, in the spatial analysis, has the potential to stimulate growth, as mean Basal Area Increment increase from colder to warmer sites. Similarly, monthly temperature, in the temporal analysis, showed a positive relationship with the growth rate. Higher mean temperature during the middle of the current growing season leads to higher annual growth rates. It is also clear from the results of the temporal analysis that higher temperatures during the previous growing season result in a reduced annual growth rate. This negative effect of previous climate conditions on the growth of trees is usually associated with the dynamics of Non-Structural Carbohydrates (NSC) (Locosselli and Buckeridge, 2017), and the higher growth rates stimulated by warmer years may lead to a reduction in NSC reserves to be used in the next growing season.

The positive relationship between growth rate and either surface temperature or mean monthly temperature suggests that growth rate may be limited by relatively lower temperatures. These results may represent a direct effect of temperature on the growth of trees, because their physiology benefits from higher temperatures up to a certain

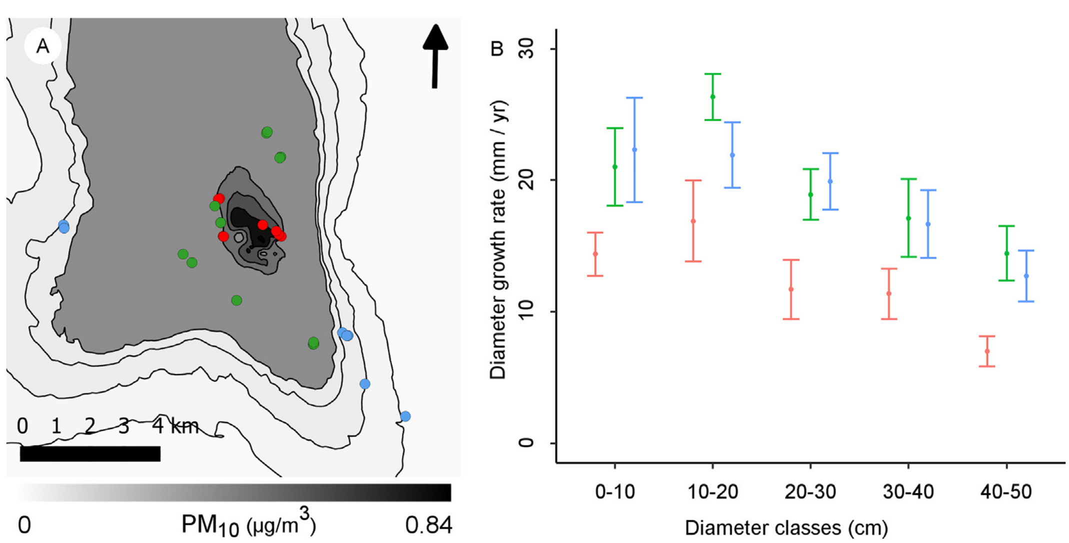

Fig. 3. Effect of the air pollution produced by the industrial cluster. A) exposure of the sampled *Tipuana tipu* trees to the modeled PM_{10} emissions from the industrial cluster (isolines): high, medium and low exposures (red, green and blue, respectively). The arrow indicates the North. The model output represents the average concentration of the last 24 h in each point of the map only from the industrial activities. B) Diametric growth rate (circles represents the mean and the bars represents the standard errors) of *Tipuana tipu* tree by diameter classes.

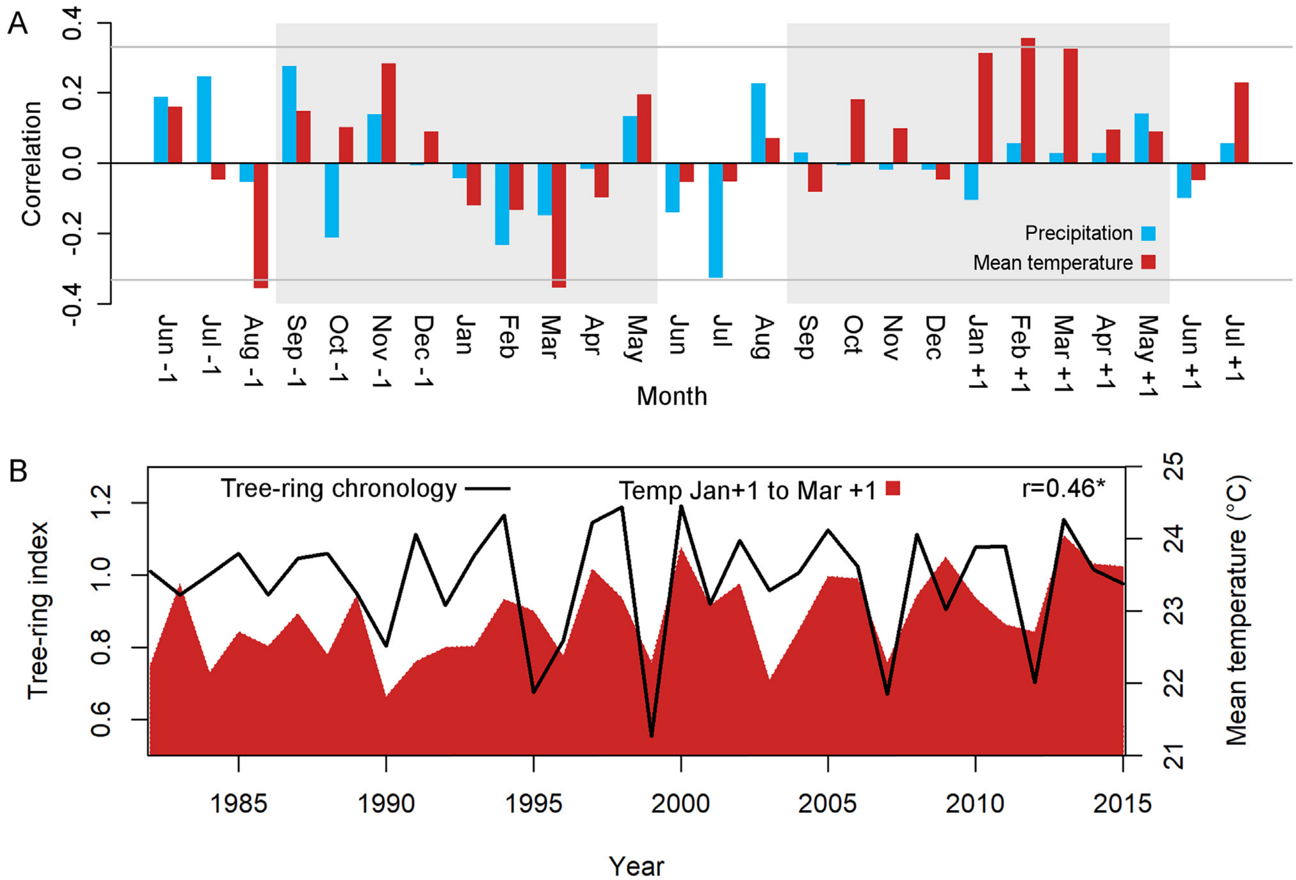

Fig. 4. Climate growth relationships for *Tipuana tipu*. A) Correlations between the tree-ring chronology and monthly mean temperature (red) and precipitation (blue) for the period between 1982 and 2015. The grey lines indicate $\alpha = 0.05$, and the correlation bars that cross the grey lines indicate statistically significant correlation values. The grey areas represent the month with precipitation higher than 60 mm. B) Correlation between mean temperature of the period from January to March of the current growth season and the tree-ring chronology. * statistically significant for $\alpha = 0.05$.

level (Ryan, 2010; Way and Oren, 2010). Otherwise, these results are a consequence of the association between temperature and light availability (Graham et al., 2003). At the spatial dimension, temperature and light availability decrease as a result of the shadows created by the taller trees from green areas (Yu and Hien, 2006; Sodouvi et al., 2018) and by taller buildings (Small, 2006). From the temporal point of view, temperature and the light availability required for photosynthesis are affected by cloud cover (Warren et al., 2007).

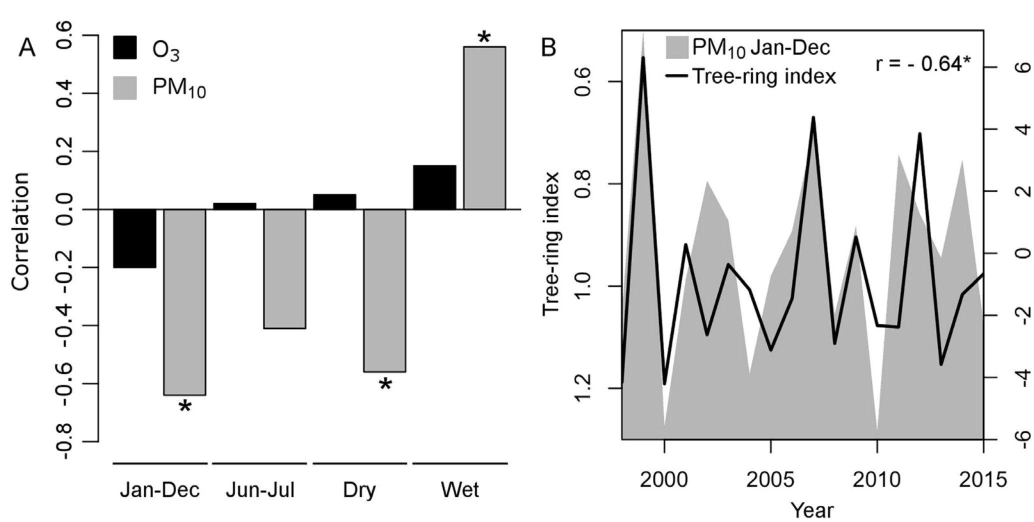

Fig. 5. Effect of interannual pollution variability in the growth of *T. tipu*. A) Correlation values between the tree-ring chronology of *Tipuana tipu* and the annual concentrations (Jan-Dec) of ozone (O_3) and particulate matter (PM_{10}) series from Santo André - Capuava (CETESB). The asterisks indicate statistically significant correlations for $\alpha = 0.05$. Correlations were calculated for calendar year (Jan - Dec), growth year (Jun – Jul + 1), six driest months (Apr – Sep) and, six wettest years (Oct – Apr + 1). B) Comparison between the standard tree-ring chronology (inverted axis) and the residuals of the spline fit for the mean annual PM_{10} concentrations.

Table 5
Least-square linear models that explain the role of climate and air pollution in the inter-annual growth varibility of *Tipuana tipu*. Model selection was based on the second orded Akiake's Information Criteria value (AICc). Models are considered distinct if the difference in the values of the AICc are equal or higher than 2. The best model has the lowest AICc value (in bold). The description of the best model shows the coefficient estimates, the standard error (Std error), sum of squares, explained percentage and the respective p values.

Model selection	
Models	AICc
Tree-ring index = Temp (Jan + 1 to Mar + 1) + PM_{10}	−15.68
Tree-ring index = PM_{10}	−13.21
Tree-ring index = Temp (Jan +1 to Mar +1)	−13.19

Best model description

$R^2 = 0.57$, $p = 0.002$

	Coefficients	Std error	Sum square	Exp. percentage	p
Intercept	−2.28	1.36	–	–	0.11
PM_{10}	−0.02	0.01	0.23	41%	0.002
Temp (Jan +1 - Mar +1)	0.14	0.06	0.09	16%	0.030
Residuals	–	–	0.24	43%	–

Our results also show that air pollution plays a role in the growth rate of urban trees. Out of all chemical elements measured in the bark of trees to characterize spatial variability of airborne pollution, the following elements Al, Ba and Zn are negatively associated with trees growth. Aluminum is a known toxic element for plants and has the potential to limit their growth by affecting both physiology and morphology. Higher concentrations of aluminum interfere in the development of roots, uptake of essential nutrients like P, enzyme functioning, to name but a few (Grout et al., 2001). Although zinc is a micronutrient present in various plant proteins, it can be toxic at the elevated concentrations found in urban environments (Broadley et al., 2007). These chemical elements are related to the wear out of vehicular spares (Moreira et al., 2016), which is usually higher in areas with higher traffic intensity, such as busy avenues (Moreira et al., 2016, 2018).

On the other hand, Ba phytotoxicity is considerably low (Llugany et al., 2000), but is a reliable indicator of vehicular emissions (Monaci and Bargagli, 1997; Monaci et al., 2000; Fernández-Espinoza and Ternero-Rodríguez, 2004) which contain other chemical elements such as Zn and Al. Despite the negative effect of Al, Ba and Zn, the growth of these trees benefited from higher concentrations of P, which is associated with biomass burning (Moreira et al., 2016). Phosphorus is a known macronutrient of plants. It is the basis of all energy metabolism (photosynthesis and respiration) and also a vital element of the structure of nucleic acid molecules.

Our results also show an effect of the industrial cluster on the growth of *T. tipu* trees. The modeled dispersion of PM_{10} suggests that industrial activity negatively affects their growth rate. There is an overall trend of growth reduction in the trees under higher exposure to PM_{10}. Trees tend to accumulate particulate matter in the leaf surface (Saebo et al., 2012), where it changes leaves optical properties, increasing their temperature and reducing light availability for photosynthesis (Grantz et al., 2003; Prajapati, 2012). It may also reduce gas exchanges due to accumulation on leaf stomata (Grantz et al., 2003, Prajapati, 2012); furthermore, the alkaline and acid substances found in PM_{10} may cross the epidermis affecting the mesophyll (Grantz et al., 2003).

Levels of PM_{10} concentrations also modulates the inter-annual growth rates of *T. tipu* trees. Higher concentrations of PM_{10} from January to December are associated with lower annual growth rates. The deposition and accumulation of PM_{10} in the leaves during low precipitation periods is probably affecting the accumulation of non-structural carbohydrates during the end of the past growing season and affecting photosynthesis during the beginning of the current growth season (Locosselli and Buckeridge, 2017). The relationship between the growth rate of *T. tipu* and PM_{10} may become positive during the rainy months, when most particulate matter is washed-off from the atmosphere and surface of leaves and made available in the soil. As highlighted before, chemical elements found in air pollution, like P, are readily uptaken by the roots, favoring their growth rates. The high variability of PM_{10} observed in the Metropolitan Region of São Paulo can be associated with annual fuel production and use of either gasoline (higher particulate matter emission) or ethanol (lower particulate matter emission) by the large fleet of flex-fuel vehicles (Salvo et al., 2017). In the temporal analysis, PM_{10} largely explains the inter-annual variability of growth rates of *T. tipu* when compared to temperature. The stronger effect of air pollution on the growth of urban trees is somewhat surprising, because climate is thought to be one of the main drivers of growth variability in the natural environment (Hughes, 2002), but not in cities.

Although the development of plants can be affected by O_3 (Paolletti, 2013) for being highly reactive (Heath, 2012), we found no significant correlation between O_3 and *T. tipu* growth rate. Either this species displays mechanisms to avoid or protect against O_3 as some species do (Chen and Gallie, 2005), or the measured values of O_3 used for our correlations do not reflect the real exposure to O_3, because of its high diffusibility in the atmosphere. Either way, there is no evidence of the effect of ozone on the growth rate of *T. tipu* in this part of the city.

Although cities may count on the ecosystem services provided by urban trees, their development is affected by both climate and air pollution. Despite the presence of heat island effect and lower water availability because of impervious cover, *T. tipu* trees growth benefit from warmer conditions, while they are not affected by the impervious cover and lower availability as measured by precipitation. Nonetheless, their growth rate is strongly hampered by the effects of air pollution. Impacts of air pollution on the development of trees may reduce the ecosystem services provided by them because these services increase with tree size (McPherson et al., 1994; Sydnor and Subburayalu, 2011; Mullaney et al., 2015). Therefore, air pollution may be considered as significant for the health of trees in large urban conglomerates as it is for humans' health (Cheng et al., 2016). Considering that trees provide ecosystem services that are thought to be important as adaptation measures to the climate change (de Coninck et al., 2018), an indirect negative effect of air pollution on an important adaptation tool becomes apparent.

5. Conclusion

Tipuana tipu is a potential species to be used in dendrochronological studies in cities. We used this species to evaluate how climate and air pollution affect the development of urban trees. We found that climate modulates the growth of these trees in the urban environment, with temperature positively influencing their growth. Nonetheless, air pollution (PM_{10}, and airborne Al, Ba, Zn) has a dramatic influence on tree inter-annual growth variability as compared to temperature. Current high concentrations of air pollution found in megacities may be considered a constraint to tree growth. Such limitations of tree growth may hamper the ecosystem services that could be provided by trees when used as mitigation or adaptation tools to environmental change. Measures to decrease air pollution, such as the use of biofuel, electrification of transport, and improvement of materials designed to decrease pollution by metals, could favor the maintenance, and improvement of ecosystem services provided by urban trees.

Acknowledgement

The authors thank Dr. Maria Ângela Zackarelli and the Prosecutor José Luiz Saikali for stimulating the study and for providing the

authorization for sampling the trees in this area. The authors thank Fabio Machado Coelho and Rafael Santos Saraiva for helping in the field work. The authors thank Rafael Santos Saraiva and Marceli Barros Britofor helping with the trees bark analysis. This study was financed by the São Paulo Research Foundation (FAPESP 2013/21728-2, 2015/25511-3, 2017/10544-9) and by National Council for Scientific and Technological Development (CNPq 304126/2015-2). This work was supported by the Instituto Nacional de Ciência e Tecnologia do Bioetanol – INCT do Bioetanol (FAPESP 2008/57908-6 and CNPq 574002/2008-1). DP (CNPq 2016/133586).

Appendix A. Supplementary data

Supplementary data to this article can be found online at https://doi.org/10.1016/j.scitotenv.2019.02.291.

References

Abreu-Harbich, L.V., Labaki, L.C., Matzarakis, A., 2015. Effect of tree planting design and tree species on human thermal confort in the tropics. Landsc. Urban Plan. 138, 99–109.

Afzali, A., Rashid, M., Afzali, M., Younesi, V., 2017. Prediction o fair pollutants concentrations from multiple sources using AERMOD coupled with WRF prognostic model. J. Clean. Prod. 166, 1216–1225.

Barsi, J.A., Barker, J.L., Schott, J.R., 2003. An atmospheric correction parameter calculator for a single thermal band earth-sensing instrument. IGARSS 2003. 2003 IEEE International Geoscience and Remote Sensing Symposium. Proceedings. 21-25, Toulouse, France.

Bartens, J., Grissino-Mayer, H., Day, S.D., Wiseman, P.E., 2012. Evaluating the potential for dendrochronological analysis of live oak (*Quercus virginiana* Mill.) from the urban and rural environment – an explorative study. Dendrochronologia 30 (1), 15–21.

Brandt, L., Lewis, A.D., Fahey, R., Scott, L., Darling, L., Sawnston, C., 2016. A framework for adapting urban forests to climate change. Environ. Sci. Pol. 66, 393–402.

Breuste, J.H., 2013. Investigations of the urban street tree forest of Mendoza, Argentina. Urban Ecosyst. 16, 801–818.

Brienen, R.J.W., Zuidema, P.A., 2005. Relating tree growth rainfall in Bolivian rain forest: a test for six species using tree-ring analysis. Oecologia 146, 1–12.

Broadley, M.R., White, P.J., Hammond, J.P., Zelko, I., Lux, A., 2007. Zinc in plants. New Phytol. 173, 677–702.

Buckeridge, M.S., 2015. Árvores urbanas em São Paulo: planejamento, economia e água. Estudos Avançados 29, 85–101.

Chen, Z., Gallie, D.R., 2005. Ascorbic acid confers greater protection against zone than increasing avoidance. Plant Physiol. 138, 1673–1689.

Cheng, Z., Luo, L., Wang, S., Wang, Y., Sharma, S., Shimadera, H., Zhou, W., 2016. Status and characteristics of ambient PM 2.5 pollution in global megacities. Environ. Int. 89, 212–221.

Cocozza, C., Ravera, S., Cherubini, P., Lombardi, F., Marchetti, M., Tognetti, R., 2016. Integrated biomonitoring of airborne pollutants over space and time using tree rings, bark, leaves and epiphytic lichens. Urban For. Urban Green. 17, 177–191.

Cook, E.R., Holmes, R.L., 1996. Guide for computer program ARSTAN. In: Grissino-Mayer, H.D., Holmes, R.L., Fritz, H.C. (Eds.), The international tree-ring Data Bank Program Library version 2.0 User's Manual. University of Arizona, Tucson.

Cook, E.R., Kairiukstis, L., 1990. Methods of Dendrochronology: Applications in the Environmental Science. Springer, Berlin.

de Coninck, H., Revi, A., Babiker, M., Bertoldi, P., Buckeridge, M., Cartwright, A., Dong Ford, W.J., Fuss, S., Hourcade, J.C., Ley, D., Mechler, R., Newman, P., Revokatova, A., Schultz, S., Steg, L., Sugiyama, T., 2018. Strengthening and implementing the global response. Global Warming of 1.5°C. An IPCC Special Report on the Impacts of Global Warming of 1.5°C Above Pre-industrial Levels and Related Global Greenhouse Gas Emission Pathways, in the Context of Strengthening the Global Response to the Threat of Climate Change, Sustainable Development, and Efforts to Eradicate Poverty [V. Masson-Delmotte, P. Zhai, H. O. Pörtner, D. Roberts, J. Skea, P.R. Shukla, A. Pirani, W. Moufouma-Okia, C. Péan, R. Pidcock, S. Connors, J. B. R. Matthews, Y. Chen, X. Zhou, M. I. Gomis, E. Lonnoy, T. Maycock, M. Tignor, T. Waterfield (eds.)]. Intergovernmental Panel on Climate Change (IPCC), Geneva, Switzerland.

Escobedo, F.J., Nowak, D.J., 2009. Spatial and air pollution removal by an urban forest. Landsc. Urban Plan. 90, 102–110.

Faraway, J.J., 2005. Linear Models. Chapman & Hall/CRC, Boca Raton.

Fernández-Espinoza, A.J., Ternero-Rodríguez, M., 2004. Study of traffic pollution by metals in Seville (Spain) by physical and chemical speciation methods. Anal. Bioanal. Chem. 379, 684–699.

Gillner, S., Bräuning, A., Roloff, A., 2014. Dendrochronological analysis of urban trees: climatic response and impact of drought on frequently used tree species. Trees Struct. Funct. 28 (4), 1079–1093.

Graham, E.A., Mulkey, S.S., Kitajuma, K., Phillips, N.G., Wright, S.J., 2003. Cloud cover limits net CO2 uptake and growth of a rainforest tree during tropical rainy seasons. Proc. Natl. Acad. Sci. 100, 572–576.

Grantz, D.A., Garner, J.H.B., Johnson, D.W., 2003. Ecological effects of particulate matter. Environ. Int. 29 (2–3), 213–239.

Grout, G.R., Samantaray, S., Das, P., 2001. Aluminum toxicity in plants: a review. Agronomie 21, 3–21.

Heath, R.L., 2012. Ozone. In: Mudd, Jb, Kozlowski (Eds.), Responses of Plants to Air Pollution. Academic Press (383 pp).

Hietz, P., 2011. A simple program to measure and analyze tree rings using excel, R and SigmaScan. Dendrochronologia 29, 245–250.

Holmes, R.L., 1993. Computer-assisted quality control in tree-ring dating and measurement. Tree-Ring Bull. 43, 69–78.

Hughes, M.K., 2002. Dendrchronology in climatology – the state of art. Dendrochronologia 20, 95–116.

Hunt, Watkiss, P., 2011. Climate change impacts and adaptation in cities: a review of the literature. Clim. Chang. 104 (1), 13–49.

Kumar, A., Patil, R.S., Dikshit, A.K., Islam, S., Kumar, R., 2016. Evaluation of control strategies for insdustrial air pollution sources using American Metereological Society/Environmental Protection Agency Regulatory Model with simulated metereology by Weather Reaserch and Forecasting Model. J. Clean. Prod. 116, 110–117.

Kuruneri-Chitepo, C., Shackleton, C.M., 2011. The distribution, abundance and composition of street trees in selected towns of the Eastern Cape, South Africa. Urban For. Urban Green. 10, 247–254.

Legumes, 2017. Version 10.38 20 July 2010-Scientific Names: *Tipuana tipu* (Benth.) Kuntze. Available online at:. http://www.legumes-online.net/ildis/aweb/td006/td_01183.htm, Accessed date: 13 December 2017.

Livesley, S.J., McPherson, E.G., Calfapietra, C., 2016. The urban forest and ecosystem service: impacts on urban water, heat, and pollution cycles at the tree, street and city scale. J. Environ. Qual. 45, 119–124.

Llugany, M., Poschenrieder, C., Barceó, J., 2000. Assessment of barium toxicity in bush beans. Arch. Environ. Contam. Toxicol. 39, 440–444.

Locosselli, G.M., Buckeridge, M.S., 2017. Dendrobiochemistry, a missing link to futher understand carbon allocation during growth and decline of tree. Trees Struct. Funct. 31 (6), 1745–1758.

Locosselli, G.M., Chacón-Madrid, K., Arruda, M.A.Z., Camargo, E.P., Moreira, T.C., André, C.D.S., André, P.A., Singer, J.M., Saldiva, P.H.N., Buckeridge, M.S., 2018. Tree rings reveal the reduction of Cd, Cu, Ni and Pb pollution in the central region of São Paulo, Brazil. Environ. Pollut. 242, 320–328.

Manes, F., Incerti, G., Salvatori, E., Vitale, M., Ricotta, C., Costanza, R., 2012. Urban ecosystem services: tree diversity and stability of tropospheric ozone removal. Ecol. Appl. 22, 349–360.

Mazerolle, M.J., 2017. AICcmodavg: model selection and multimodel inference based on (Q)AIC(c). R package version 2.1-1. https://cran.r-project.org/package=AICcmodavg.

Mazza, M., Refojo, N., Bosco-Borgeat, M.E., Taverna, C.G., Trovero, A.C., Rogé, A., Davel, G., 2013. *Cryptococcus gattii* in urban trees from cities in North-eastern Argentina. Mycoses 56, 645–650.

McPherson, E.G., Nowak, D.J., Rowntree, R.A., 1994. Chicago's urban forest ecosystem: results of the Chicago urban forest climate project. USDA Forest Service Northeastern Forest Experiment Station General Technician Report: NE-186.

Monaci, F., Bargagli, R., 1997. Barium and other trace metals as indicators of vehicle emission. Water Air Soil Pollut. 100, 89–98.

Monaci, F., Moni, F., Lanciotti, E., Grechi, D., Bargagli, R., 2000. Biomonitoring of airborne metals in urban environments: new tracers of vehicle emissions, in place of lead. Environ. Pollut. 107, 321–327.

Moreira, T.C.L., Oliveira, R., Amato, L.F.L., Kang, C., Saldiva, P.H.N., Saiki, M., 2016. Intra-urban biomonitoring: source apportionment using tree barks to identify air pollution sources. Environ. Int. 91, 271–275.

Moreira, T.C.L., Lourenço, L.F.A., Silva, G.T., André, C.D.S., André, P.A., Barrozo, L.V., Singer, J.M., Saldiva, P.H.N., Saiki, M., Locosselli, G.M., 2018. The use of tree barks to monitor traffic related air pollution: a case of study in São Paulo-Brazil. Front. Environ. Sci. 6, 72. https://doi.org/10.3389/fenvs.2018.00072.

Mullaney, J., Lucke, T., Trueman, S.J., 2015. A review for benefits and challenges in growing street trees in paved environments. Landsc. Urban Plan. 134, 157–166.

Nowak, D.J., Greenfield, E.J., Hoehn, R.E., Lapoint, E., 2013. Carbon storage and sequestration by trees in urban and community areas of the United States. Environ. Pollut. 178, 229–236.

Ordóñez, C., Duinker, P.N., 2014. Assessing the vulnerability of urban forests to climate change. Environ. Rev. 22, 311–321.

Paolletti, E., 2013. Ozone and urban forests in Italy. Environ. Pollut. 1506–1512.

Peters, R.L., Groenendijk, P., Vlam, M., Zuidema, P.A., 2015. Detecting long-term growth trends using tree rings: a critical evaluation of the methods. Glob. Chang. Biol. 21, 2040–2054.

Prajapati, S.K., 2012. Ecological effect of airborne particulate matter on plants. Environmental Skeptics and Critics. 1, pp. 12–22.

R Core Team, 2017. R: A Language and Environment for Statistical Computing. R Foundation for Statistical Computing, Vienna, Austria URL. https://www.R-project.org/.

Ryan, M.G., 2010. Temperature and tree growth. Tree Physiol. 30, 667–668.

Saebo, A., Popek, R., Nawrot, B., Hanslin, H.M., Gawronska, H., Gawronska, S.W., 2012. Plant species differences in particulate matter accumulation on leaf surfaces. Sci. Total Environ. 427-428, 347–354.

Salvo, A., Brito, J., Artaxo, P., Geiger, F.M., 2017. Reduced ultrafine particle levels in São Paulo's atmosphere during shifts from gasoline to etanol use. Nat. Commun. https://doi.org/10.1038/s41467-017-00041-5.

Sashua-Bar, L., Potchter, O., Bitan, A., Boltansky, D., Yaakov, Y., 2010. Microclimate modelling of street tree species effects within the varied urban morphology in the Mediterranean city of Tal Avivi, Israel. Int. J. Climatol. 30, 44–47.

Schneider, C.A., Rasband, W.S., Eliceiri, K.W., 2012. NIH image to ImageJ: 25 years of image analysis. Nat. Methods 9 (7), 671–675.

Schweingruber, F.H., 1988. Tree Rings. Basics and Applications of Dendrochronology. Kluwer, Dordrecht.

Sicard, P., Agathokleous, E., Araminiene, V., Carrari, E., Hoshika, Y., De Marco, A., Paoletti, E., 2018. Should we see urban trees as effective solutions to increasing ozone levels in cities? Environ. Pollut. 243, 163–176.
Small, C., 2006. Comparative analysis of urban reflectance and surface temperature. Remote Sens. Environ. 104 (2), 168–189.
Smardon, R.C., 1988. Perception and aesthetics of the urban environment: review of the role of vegetation. Landsc. Urban Plan. 15, 85–106.
Soares, Al, Rego, F.C., McPherson, E.G., Simpson, J.R., Peper, P.J., Xiao, Q., 2011. Benefits and costs of street trees in Lisbon, Portugal. Urban For. Urban Green. 10, 69–70.
Sodouvi, S., Zhang, H., Chi, X., Müller, F., Li, H., 2018. The influence of spatial configuration of green areas on microclimate and thermal comfort. Urban For. Urban Green. 34, 85–96.
Stokes, M.A., Smiley, T.L., 2006. An introduction to Tree-ring Dating. The University of Arizona Press, Tucson, US (73 pgs).
Sydnor, T.D., Subburayalu, S.K., 2011. Should we consider expected environmental benefits when planting larger or smaller tree species. Arboricult. Urban For. 37 (4), 167–172.
Teixeira, E.T., 2014. Evaluación de la estructura y comportamiento del arbolado urbano en Motevideo. (PhD Thesis). Universidade de la República, Facultad de Agronomia, Montivideo, Uruguay (135 pg).
Torbenson, M.C.A., 2015. Dendrochronology. In: Clarke, L., Nield, J. (Eds.), Geomorphological Techiniques. British Society for Geomorphology (Chapter 4, Section 2.8).
Trouet, V., Van Oldenborgh, G.J., 2013. KNMI climate explorer: a web-based research tool for high-resolution paleoclimatology. Tree-Ring Res. 69 (1), 3–13.
United Nations, Department of Economic and Social Affairs, Population Division, 2018. The World's Cities in 2018 – Data Booklet (ST/ESA/SER.A/417).
USGS (United States Geological Survey), 2018. Using the USGS Landsat 8 Product. Disponível em:. https://landsat.usgs.gov/using-usgs-landsat-8-product, Accessed date: 20 January 2018.
Warren, S.G., Eastman, R.M., Hahn, C.J., 2007. A survey of changes in cloud cover and cloud types over land from surface observations, 1971-96. J. Clim. 20, 717–738.
Way, D.A., Oren, O., 2010. Differential responses to changes in growth temperature between trees from different functional groups and biomes: a review and synthesis of data. Tree Physiol. 30, 669–688.
Wigley, T.M.L., Briffa, K.R., Jones, P.D., 1984. On the average value of correlated time series with applications in dendrochronology and hydrometeorology. J. Clim. Appl. Meteorol. 23, 201–213.
Xiao, Q., McPherson, E.G., 2002. Rainfall interception by Santa Monica's municipal urban forest. Urban Ecosyst. 6, 291–302.
Yu, C., Hien, W.N., 2006. Thermal benefits of city parks. Energ. Buildings 38, 105–120.
Zaproni, Z., Biondi, D., Neto, E.M.L., Martini, A., 2013. Efeito das variáveis metereológicas sobre a fenologia de *Tipuana tipu* (Benth.) O. Kuntze na arborização urbana de Curitiba-Pr. REVSBAU 8. pp. 1–14.